

Parallel Implementation of the PHOENIX Generalized Stellar Atmosphere Program

Peter H. Hauschildt^{1,2}, E. Baron³, and France Allard⁴

Received _____; accepted _____

¹Dept. of Physics and Astronomy, University of Georgia, Athens, GA 30602-2451;
yeti@hal.physast.uga.edu

²Dept. of Physics and Astronomy, Arizona State University, Tempe, AZ 85287-1504

³Dept. of Physics and Astronomy, University of Oklahoma, 440 W. Brooks, Rm 131,
Norman, OK 73019-0225; baron@phyast.nhn.ou.edu

⁴Dept. of Physics, Wichita State University, Wichita, KS 67260-0032;
allard@eureka.physics.twsu.edu

ABSTRACT

We describe the parallel implementation of our generalized stellar atmosphere and NLTE radiative transfer computer program PHOENIX. We discuss the parallel algorithms we have developed for radiative transfer, spectral line opacity, and NLTE opacity and rate calculations. Our implementation uses a MIMD design based on a relatively small number of MPI library calls. We report the results of test calculations on a number of different parallel computers and discuss the results of scalability tests.

1. Introduction

Much of the astrophysical information that we possess has been obtained via spectroscopy. Spectroscopy of astrophysical objects allows us to ascertain velocities, temperatures, abundances, sizes, and luminosities of astrophysical objects. Much can be learned from some objects just by examining line ratios and redshifts, but to really understand an observed spectrum in detail often requires detailed fits to synthetic spectra. Detailed synthetic spectra also serve to test theoretical models for various astrophysical objects. Since many astrophysical objects of interest feature relativistic flows (e.g., supernovae, novae, and accretion disks), low electron densities (e.g., supernovae and novae), and/or molecular formation (e.g., cool stars, brown dwarfs, and giant planets), detailed models must include special relativistic effects and a very large number of ions and molecules in the equation of state in order to make quantitative predictions about, e.g., abundances. In addition, deviations from local thermodynamic equilibrium (LTE) must be considered to correctly describe the transfer of radiation and the emergent spectrum.

We have developed the spherically symmetric special relativistic non-LTE generalized radiative transfer and stellar atmosphere computer code **PHOENIX** (Hauschildt 1992, 1993; Hauschildt & Baron 1995; Hauschildt et al. 1995; Allard & Hauschildt 1995; Hauschildt et al. 1996; Baron et al. 1996) which can handle very large model atoms as well as line blanketing by millions of atomic and molecular lines. This code is designed to be very flexible, it is used to compute model atmospheres and synthetic spectra for, e.g., novae, supernovae, M and brown dwarfs, white dwarfs and accretion disks in Active Galactic Nuclei (AGN); and it is highly portable. When we include a large number of line transitions, the line profiles must be resolved in the co-moving (Lagrangian) frame. This requires many wavelength points, (we typically use 50,000 to 150,000 wavelength points). Since the CPU time scales linearly with the number of wavelength points the CPU time requirements

of such a calculation are large. In addition, each NLTE radiative rate for both line and continuum transitions must be calculated and stored at every spatial grid point which requires large amounts of storage and can cause significant performance degradation if the corresponding routines are not optimally coded.

In order to take advantage of the enormous computing power and vast memory sizes of modern parallel supercomputers, both potentially allowing much faster model construction as well as more detailed models, we have implemented a parallel version of **PHOENIX**. Since the code uses a modular design, we have implemented different parallelization strategies for different modules in order to maximize the total parallel speed-up of the code. In addition, our implementation allows us to change the load distribution onto different nodes both via input files and dynamically during a model run, which gives a high degree of flexibility to optimize the performance on a number of different machines and for a number of different model parameters.

Since we have both large CPU and memory requirements we have initially implemented the parallel version of the code on the **IBM SP2** using the **MPI** message passing library (Message Passing Interface Forum 1995). Since the single processor speed of the **IBM SP2** is high, even a small number of additional processors can lead to significant speed-up. We have chosen to work with the **MPI** message passing interface, since it is both portable (public domain implementations of **MPI** are readily available cf. Gropp et al. 1996), running on dedicated parallel machines and heterogeneous workstation clusters and it is available for both distributed and shared memory architectures. For our application, the distributed memory model is in fact easier to code than a shared memory model, since then we do not have to worry about locks and synchronization, etc. on *small* scales and we, in addition, retain full control over interprocess communication. This is especially clear once one realizes that it is fine to execute the same code on many nodes as long as it is not too CPU

intensive, and avoids costly communication,

An alternative to an implementation with `MPI` is an implementation using High Performance Fortran (`HPF`) directives (in fact, both can co-exist to improve performance). However, the process of automatic parallelization guided by the `HPF` directives is presently not yet generating optimal results because the compiler technology is still very new. In addition, `HPF` compilers are not yet widely available and they are currently not available for heterogeneous workstation clusters. `HPF` is also more suited for problems that are purely data-parallel (SIMD problems) and would not benefit much from a MIMD approach. An optimal `HPF` implementation of `PHOENIX` would also require a significant number of code changes in order to explicitly instruct the compiler not to generate too many communication requests, which would slow down the code significantly. The `MPI` implementation requires only the addition of a few explicit communication requests, which can be done with a small number of library calls.

2. Basic numerical methods

The co-moving frame radiative transfer equation for spherically symmetric flows can be written as (cf. Mihalas & Mihalas 1984):

$$\begin{aligned}
& \gamma(1 + \beta\mu) \frac{\partial I_\nu}{\partial t} + \gamma(\mu + \beta) \frac{\partial I_\nu}{\partial r} \\
& + \frac{\partial}{\partial \mu} \left\{ \gamma(1 - \mu^2) \left[\frac{1 + \beta\mu}{r} \right. \right. \\
& \quad \left. \left. - \gamma^2(\mu + \beta) \frac{\partial \beta}{\partial r} - \gamma^2(1 + \beta\mu) \frac{\partial \beta}{\partial t} \right] I_\nu \right\} \\
& - \frac{\partial}{\partial \nu} \left\{ \gamma \nu \left[\frac{\beta(1 - \mu^2)}{r} + \gamma^2 \mu(\mu + \beta) \frac{\partial \beta}{\partial r} \right. \right. \\
& \quad \left. \left. + \gamma^2 \mu(1 + \beta\mu) \frac{\partial \beta}{\partial t} \right] I_\nu \right\} \\
& + \gamma \left\{ \frac{2\mu + \beta(3 - \mu^2)}{r} \right. \\
& \quad \left. + \gamma^2(1 + \mu^2 + 2\beta\mu) \frac{\partial \beta}{\partial r} + \gamma^2[2\mu + \beta(1 + \mu^2)] \frac{\partial \beta}{\partial t} \right\} I_\nu \\
& = \eta_\nu - \chi_\nu I_\nu.
\end{aligned} \tag{1}$$

We set $c = 1$; β is the velocity; and $\gamma = (1 - \beta^2)^{-1/2}$ is the usual Lorentz factor. Equation 1 is a integro-differential equation, since the emissivity η_ν contains J_ν , the zeroth angular moment of I_ν :

$$\eta_\nu = \kappa_\nu S_\nu + \sigma_\nu J_\nu,$$

and

$$J_\nu = 1/2 \int_{-1}^1 d\mu I_\nu,$$

where S_ν is the source function, κ_ν is the absorption opacity, and σ_ν is the scattering opacity. With the assumption of time-independence $\frac{\partial I_\nu}{\partial t} = 0$ and a monotonic velocity field Eq. 1 becomes a boundary-value problem in the spatial coordinate and an initial value problem in the frequency or wavelength coordinate. The equation can be written in operator form as:

$$J_\nu = \Lambda_\nu S_\nu, \tag{2}$$

where Λ is the lambda-operator.

3. Machines used for testing

We were able to test the algorithms described here on a few different machines. In this section we describe briefly the characteristics of each system for reference. There are significant differences between the architectures of the various systems, so we could test the behavior of the code under very different conditions.

3.1. IBM SP2

The IBM SP2 is a distributed memory machine based on the IBM Power2 chipset. Each node is, effectively, an independent workstation with its own operating system, paging space, and local disk space. The nodes are connected in a flat topology, with a high-speed crossbar switch that has a peak performance of 30 MB/s. We ran tests on the IBM SP2's of the University of Oklahoma and the Cornell Theory Center equipped with 62.5 MHz "thin-node 2" nodes with 128 to 512 MB memory, \geq 1 GB local disk space. In addition, both IBM SP2's have a parallel filesystem (PIOFS) that allows parallel IO to improve performance.

3.2. HP J200

We were able to run a number of tests on a dual processor HP J200. This machine is a SMP design with two HP PA-7200 processors running at 100 MHz. Our test machine has 128MB of memory and a fast 3GB scratch filesystem. We use the public domain MPI implementation MPICH (Gropp et al. 1996) compiled on this machine and the HP Fortran compiler and libraries for the test calculations.

3.3. Parsytec GigaClusters

We have run tests of the radiative transfer code on two **Parsytec GigaClusters** of the Paderborn Center for Parallel Computing (**PC**²). We could not yet run tests with **PHOENIX** because of memory and disk limitations on these machines, but the radiative transfer calculations give an indication on the performance and scalability of these systems.

3.3.1. GC/PP

The **Parsytec GigaCluster Power Plus** (**GC/PP**) uses PowerPC 601 CPU's at a clockspeed of 80 MHz. Each processor has a peak performance of 80 MFlops and a LINPACK 100x100 performance of 15 MFlops. The machine of the **PC**² has 64 MB memory per processing element (2 CPU's). The communication between processors has a peak performance of 20 MB/s, but the sustained performance is only 3.3 MB/s. The **GC/PP** runs under **PARIX 1.3.1** and uses the **Motorola** Fortran compiler and **PC**²'s version of the **MPI** libraries.

3.3.2. GCel

The **GCel** uses T805 transputer CPU's at a clockspeed of 30 MHz. Each transputer has a peak performance of 4.3 MFlops and a LINPACK 100x100 performance of 0.63 MFlops. The **GCel** of the **PC**² has 4 MB memory per node. The communication between processors has a sustained performance of 8.8 MB/s. The **GCel** runs under **PARIX 1.2** and uses the **ACE** Fortran compiler and **PC**²'s version of the **MPI** libraries.

4. Parallel radiative transfer

4.1. Strategy and implementation

We use the method discussed in Hauschildt (1992) for the numerical solution of the special relativistic radiative transfer equation (RTE) at every wavelength point (see also Hauschildt, Störzer, & Baron 1994). This iterative scheme is based on the operator splitting approach. The RTE is written in its characteristic form and the formal solution along the characteristics is done using a piecewise parabolic integration (PPM, this is the “short characteristic method” Olson & Kunasz 1987). We use the exact band-matrix subset of the discretized Λ -operator as the ‘approximate Λ -operator’ (ALO) in the operator splitting iteration scheme (see Hauschildt, Störzer, & Baron 1994). This has the advantage of giving very good convergence and high speed-up when compared to diagonal ALO’s.

The serial radiative transfer code has been optimized for superscalar and vector computers and is numerically very efficient. It is therefore crucial to optimize the ratio of communication to computation in the parallel implementation of the radiative transfer method. In terms of CPU time, the most costly parts of the radiative transfer code are the setup of the PPM interpolation coefficients and the formal solutions (which have to be performed in every iteration). The construction of a tri-diagonal ALO requires about the same CPU time as a single formal solution of the RTE and is thus not a very important contributor to the total CPU time required to solve the RTE at every given wavelength point.

In principle, the computation of the PPM coefficients does not require any communication and thus could be distributed arbitrarily between the nodes. However, the formal solution is recursive along each characteristic. Within the formal solution, communication is only required during the computation of the mean intensities J , as they involve integrals over the angle μ at every radial point. Thus, a straightforward and efficient way to parallelize the radiative transfer code is to distribute sets of characteristics

onto different nodes. This will minimize the communication during the iterations, and thus optimize the performance. Within one iteration step, the current values of the mean intensities need to be broadcast to all radiative transfer nodes and the new contributions of every radiative transfer node to the mean intensities at every radius must be sent to the master node. The master radiative transfer node then computes and broadcasts an updated J vector using the operator splitting scheme, the next iteration begins, and the process continues until the solution is converged to the required accuracy. The setup, i.e., the computation of the PPM interpolation coefficients and the construction of the ALO, can be parallelized using the same method and node distribution. The communication overhead for the setup is roughly equal to the communication required for a single iteration.

An important point to consider is the load balancing between the N_{RT} radiative transfer nodes. The workload to compute the formal solution along each characteristic is proportional to the number of intersection points of the characteristic with the concentric spherical shells of the radial grid (the ‘number of points’ along each characteristic). Therefore, if the total number of points is N_{P} , the optimum solution would be to let each radiative transfer node work on $N_{\text{P}}/N_{\text{RT}}$ points. This optimum can, in general, not be reached exactly because it would require splitting characteristics between nodes (which involves both communication and synchronization). A simple load distribution based on $N_{\text{C}}/N_{\text{RT}}$, where N_{C} is the total number of characteristics, is far from optimal because the characteristics do not have the same number of intersection points (consider tangential characteristics with different impact parameters). We therefore chose a compromise of distributing the characteristics to the radiative transfer nodes so that the total number of points that are calculated by each node is roughly the same and that every node works on a different set of characteristics.

4.2. Performance and scalability

Following the outline given in the previous paragraphs, we have adapted the serial version of our radiative transfer code using the MPI libraries. The additions required to implement the parallel version were relatively small and required only the addition of the MPI subroutine calls. The total number of MPI statements in the radiative transfer code is 220, which is very small compared to a total of 10,700 statements.

We test the performance and scalability of the parallel radiative transfer code with a simple single wavelength radiative transfer model on an IBM SP2. The test model uses 128 radial points, we have chosen the following test parameters: the radial extension is a factor of 10, the total optical depth is 100, the ratio of absorptive to total opacity is $\epsilon = 10^{-4}$, and we require as convergence criterion that changes in the mean intensities are less than 10^{-8} between consecutive iterations (which requires 17 iterations starting with $J = B$). For simplicity, a static model is used, the tests of the full PHOENIX code described below will employ test models with velocity fields. In table 1a we list the results of test runs with different number of nodes.

The scaling of the radiative transfer code is acceptable as the number of nodes rises to about 8 nodes. More nodes do not decrease the wall-clock time significantly because the rapidly increasing communication overhead (the J must be broadcast to all nodes and the results must be gathered from all nodes in every radiative transfer iteration) as well as the worsening of the load balance (the latter becomes more acute as the number of nodes increases to ≥ 16). We have verified that the individual modules of the radiative transfer code (i.e., PPM coefficients, ALO computation, and formal solution) indeed scale with the number of nodes, within the limits of the load balancing described above. In test calculations we found that the time for either the gathering of the results of the formal solution (using MPI_REDUCE) or the broadcast of the updated J (using MPI_BCAST)

individually do not require significant amount of time. However, the *combination* of these two communications use much more time than would be predicted by the sum of the times for the individual operations. This is probably partly due to the required synchronization but also partly due to limitations of the MPI implementation and the communication hardware of the IBM SP2.

Table 1a also shows the results obtained on the GC/PP for the same test case for comparison. On a single CPU, the GC/PP is about a factor of 4.5 slower than a single CPU of the IBM SP2, which is consistent with their LINPACK results. The scaling of the GC/PP with more nodes is about the same as for the IBM SP2, indicating that the slower communication speed of the GC/PP does not produce performance problems if the number of CPU's is small. In Table 1a we also include the results for the HP J200. The speed-up for 2 CPU's is only 30%, which is due to the slower communication caused by a non-optimized MPI library.

The radiative transfer test problem with 128 radial grid-points was too large to fit into the memory of a single transputer node of the GCel without major changes in the code (which would be very time consuming because of the lack of a Fortran 90 compiler for both Parsytec systems). Therefore, we have also run a smaller test case with 50 radial gridpoints. The results are also listed in Table 1b. The performance ratio of the results on a single CPU is, as in the previous case, comparable to the ratio of the LINPACK results: The code runs about a factor of 31 faster on a single PPC 601 CPU than on the T805 transputer. However, there are now major differences in the scalability between the two systems. Whereas the scaling of the GCel results are slightly better than the results obtained for the IBM SP2 with the large test case, the wall-clock times do not scale well for both the IBM SP2 and the GC/PP, in contrast to its behavior in the large test case. The reason is the relatively slower communication (compared to raw processor speed) of the IBM SP2 and the GC/PP: in

the large test case the floating point operations dominate over the communication. For the **GCe1** with lower floating point performance but faster communication than the other two machines, the scaling to more processors is much better and comparable to the large test case for the **IBM SP2** and **GC/PP**. This demonstrates that flexibility of the load distribution is very important in order to obtain good performance on a number of different machines.

5. Parallelization of the line opacity calculation

The contribution of spectral lines by both atoms and molecules is calculated in PHOENIX by direct summation of all contributing lines. Each line profile is computed individually at every radial point for each line within a search window (typically, a few hundred to few thousand Doppler widths or about 1000Å). This method is more accurate than methods that rely on pre-computed line opacity tables (the “opacity sampling method”) or methods based on distribution functions (the “opacity distribution function (ODF) method”). Both ODF and the opacity sampling method neglect the details (e.g., depth dependence) of the individual line profiles. This introduces systematic errors in the line opacity because the pressures on the top and the bottom of the line forming region are vastly different (several orders of magnitude in cool dwarf stars) which causes very different pressure damping and therefore differing line widths over the line forming region. In addition, the pre-computed tables require a specified and fixed wavelength grid, which is too restrictive for NLTE calculations that include important background line opacities.

In typical model calculations we find that about 1,000 to 10,000 spectral lines contribute to the line opacity (e.g., in M dwarf model calculations) at any wavelength point. Therefore, we need to calculate a large number of individual Voigt profiles at every wavelength point. The subroutines for these computations can easily be vectorized and we use a block algorithm with caches and direct access scratch files for the line data to

minimize storage requirements. A block is the number of lines stored in active memory, and the cache is the total number of blocks stored in memory. When the memory size is exceeded, the blocks are written to direct access files on disk. Thus the number of lines that can be included is not limited by RAM, but rather by disk space and the cost of I/O. This approach is computationally efficient because it provides high data and code locality and thus minimizes cache/TLB and page faults. This has proven to be so effective that model calculations with more than 15 million lines can be performed on medium sized workstations (e.g., IBM RS/6000-530 with 64MB RAM and 360MB scratch disk space). The CPU time for a single iteration for a LTE model is dominated by calculating the line opacity (50 to 90% depending on the model parameters), therefore, both the LTE atomic and molecular line opacities are good candidates for parallelization.

There are several obvious ways to parallelize the line opacity calculations. The first method is to let each node compute the opacity at N_r/N_{node} radial points, the second is to let each node work on a different subset of spectral lines within each search window. A third way, related to the second method, is to use completely different sets of lines for each node (i.e., use a global workload split between the nodes in contrast to a local split in the second method). In the following, we will discuss the advantages and disadvantages of these three methods. All three methods require only a very small amount of communication, namely a gather of all results to the master node with an `MPI_REDUCE` library call.

The first and second methods, distributing sets of radial points or sets of lines within the local (wavelength dependent) search window over the nodes, respectively, are very simple to implement. They can easily be combined to optimize their performance: if for any wavelength point the number of depth points is larger than the number of lines within the local search window, then it is more effective to run this wavelength point parallel with respect to the radial points, otherwise it is better to parallelize with respect to the lines

within the local window. It is trivial to add logic to decide the optimum method for every wavelength point individually. This optimizes overall performance with negligible overhead. The speed-up for this method of parallelization is very close to the optimum value if the total number of blocks of the blocking algorithm is relatively small ($\leq 3 \dots 5$).

However, if the total number of line blocks is larger (typically, about 10 to 20 blocks are used), the overhead due to the read operations for the block scratch files becomes noticeable and can reach 20% or more of the total wall-clock time. This is due to the fact that the ‘local parallelization’ required that each node working on the line opacities needs to read every line block, thus increasing the IO time and load to the IO subsystem by the number of nodes themselves.

An implementation of the third method, i.e., distributing the global set of lines onto the nodes, will therefore be more effective if the number of lines is large (this is the usual case in practical applications). There are a number of ways to implement this approach; however, many of them would require either significant administration and communication during the line selection procedure or a large number of individual scratch files (one for each node). The by far easiest and fastest way to implement the global distribution on the IBM SP2 is to use the Parallel IO Filesystem (PIOFS). The PIOFS has the advantage that (a) the code changes required are simple and easily reversible (for compatibility with other machines), (b) the PIOFS software allows the creation of a single file on the line selection nodes (the line selection is a process that is inherently serial and can be parallelized only by separating the atomic and molecular line selections, which although simple has not yet been implemented), (c) it allows different nodes to access distinct portions of a single file as their own ‘subfiles’, and (d) that the IO load is distributed over all IO nodes that are PIOFS servers.

Points (b) and (c) make the implementation very simple. We chose a single line as the

atomic size of the **PIOFS** file that is used to store the line-blocks and create the **PIOFS** file with N_{node} sub-files (where N_{node} is the number of nodes that will later work on the LTE line opacity). The line selection routines then set the **PIOFS** file view to the equivalent of a single direct access file with the appropriate block size. After the line selection, each of the N_{node} nodes sets the local view of the **PIOFS** file such that it ‘sees’ the $1 \dots N_{\text{node}}$ subfile, so that node N reads lines N , $N + N_{\text{node}}$, $N + 2N_{\text{node}}$, and so forth. This is equivalent to the ‘global line distribution’ method with a minimal programming effort. The advantages are not only that each node has to read only $1/N_{\text{node}}$ of the total lines but also that the IO itself is distributed both over the available **PIOFS** fileservers and over time (because the different line sets will cause the block IO operations to happen at different times). The latter is very useful and enhances the parallel performance and scalability. In addition, the process is completely transparent to the program, only 2 explicit **PIOFS** subroutine calls had to be inserted to set the ‘view’ of the **PIOFS** file to the correct value.

In Fig. 1 and Table 2 we show the performance and speed-up as function of the number of nodes for a simplified model of a very low mass star. We use an M dwarf star model with the parameters $T_{\text{eff}} = 2700$ K, $\log(g) = 5.0$, and solar abundances, appropriate for the late M dwarf VB10 (Schweitzer et al. 1996). The test model includes 226,000 atomic lines (of these, 29,000 are calculated using Voigt profiles) and 11.2 million molecular lines (with 3.6 million calculated with Voigt profiles) and uses a wavelength grid with 13,000 points. We have set the line search windows to values larger than required in order to simulate “real” model calculations (which typically use twice as many wavelength points). In addition, we set the blocksizes for the line data storage to 30,000 lines for both molecular and atomic lines and used a line data cache size of 2 (that is we store in RAM 2 blocks of 30,000 lines each). This setting is optimal for the atomic lines but the blocksizes are set to larger values (about 100,000) for the molecular lines in production models. However, the cache sizes were large enough to prevent cache thrashing.

The speed-up that we find is very good and the scaling is close to the theoretical maximum for the atomic lines (a factor of 4.5 for 5 nodes). For the molecular lines the speed-up is 4.1 for 5 nodes, a little lower than for the atomic lines. This is caused by the additional IO time required to read the line data blocks from the scratch file. Ignoring the IO time, the molecular line speed-up is 4.6, very close to the value found for the atomic lines. These results were obtained by using the parallel IO system, if we instead rely on a standard file, the IO time for the molecular lines increases by a factor of 3.2 and the speed-up for the molecular lines decreases to a factor of only 2.2 (for 5 nodes, respectively). In production runs on machines that do not have a PIOFS filesystem, we would of course use larger blocksizes for the line data arrays to minimize the IO time, we usually do this on serial machines.

6. Parallelizing NLTE calculations

Our method for iteratively solving the NLTE radiative transfer and rate equations with an operator splitting method are discussed in detail in Hauschildt (1993) and Hauschildt & Baron (1995), therefore, we present here only a brief summary. The method uses a “rate-operator” formalism that extends the approach of Rybicki & Hummer (1991) to the general case of multi-level NLTE calculations with overlapping lines and continua. We use an “approximate rate-operator” that is constructed using the exact elements of the discretized Λ -matrix (these are constructed in the radiative transfer calculation for every wavelength point). This approximate rate-operator can be either diagonal or tri-diagonal. The method gives good convergence for a wide range of applications and is very stable. It has the additional advantage that it can handle very large model atoms, e.g., we use a 617 level Fe II model atom in regular model calculations (Hauschildt et al. 1996; Baron et al. 1996).

Parallelizing the NLTE calculations involves parallelizing three different sections: the NLTE opacities, the rates, and the solution of the rate equations. In the following discussion, we consider only a diagonal approximate rate-operator for simplicity. In this case, the computation of the rates and the solution of the rate equations as well as the NLTE opacity calculations can simply be distributed onto a set of nodes without any communication (besides the gathering of the data at the end of the iteration). This provides a very simple way of achieving parallelism and minimizes the total communication overhead. The generalization to a tridiagonal approximate rate-operator is in principle straightforward, and involves only communication at the boundaries between two adjacent nodes.

It would be possible to use the other two methods that we discussed in the section on the LTE line opacities, namely local and global set of lines distributed to different nodes. However, both would involve an enormous amount of communication between the NLTE nodes because each NLTE transition can be coupled to any other NLTE transition. These couplings require that a node working on any NLTE transition have the required data to incorporate the coupling correctly. Although this only applies to the nodes that work on the NLTE rates, it would require both communication of each NLTE opacity task with each other (to prepare the necessary data) and communication from the NLTE opacity nodes to the NLTE rate nodes. This could mean that several MB data would have to be transferred between nodes at each wavelength point, which is prohibitive with current communication devices.

Another way to parallelize the NLTE calculation exploits the fact that our numerical method allows the grouping of NLTE species (elements) into separate entities. These groups do not need to communicate with each other until the end of an iteration. Thus distributing groups onto different nodes will allow very effective parallelization with

little or no communication overhead. This approach can be combined with the all the parallelization approaches discussed previously, leading to better speed-ups. In addition, it would significantly reduce the memory requirements for each node, thus allowing even larger problems to be solved. We will implement this method in later releases of PHOENIX and report the results elsewhere.

We have implemented the parallelization of the NLTE calculations by distributing the set of radial points on different nodes. In order to minimize communication, we also ‘pair’ NLTE nodes so that each node works on NLTE opacities, rates and rate equations for a given set of radial points. This means that the communication at every wavelength point involves only gathering the NLTE opacity data to the radiative transfer nodes and the broadcast of the result of the radiative transfer calculations (i.e., the ALO and the J ’s) to the nodes computing the NLTE rates. The overhead for these operations is negligible but it involves synchronization (the rates can only be computed after the results of the radiative transfer are known, similarly, the radiative transfer nodes have to wait until the NLTE opacities have been computed). Therefore, a good balance between the radiative transfer tasks and the NLTE tasks is important to minimize waiting. The rate equation calculations parallelize trivially over the layers and involve no communication if the diagonal approximate rate-operator is used. After the new solution has been computed, the data must be gathered and broadcast to *all* nodes, the time for this operation is negligible because it is required only once per model iteration.

In Fig. 2 and Table 3 we show performance results for a simplified test model with the following parameters: $T_{\text{eff}} = 20,000$ K, $\log(g) = 8.0$, and solar abundances. The background LTE line opacities have been omitted and the radiative transfer code has been run in plane parallel mode on a single node to concentrate the results on the NLTE calculation. The speed-ups are acceptable although they do not reach the theoretical maximum. This is

caused by several effects. First, the NLTE opacity calculations involve the computation of the b-f cross-section, which has not been parallelized in this version of the code. These calculations are negligible in serial mode, but they become comparatively more costly in parallel mode. The solution to this will be their parallelization, which involves significant communication at each wavelength point. This will be investigated in future work.

An important problem arises from the fact that the time spent in the NLTE routines is not dominated by the floating point operations (both the number and placement of floating point operation were optimized in the serial version of the code) but by *memory access*, in particular for the NLTE rate construction. Although the parallel version accesses a much smaller number of storage cells (which naturally reduces the wall-clock time), effects like cache and TLB misses and page faults contribute significantly to the total wall-clock time. All of these can be reduced by using Fortran-90 specific constructs in the following way: We have replaced the static allocation of the arrays that store the profiles, rates etc. used in the NLTE calculations (done with **COMMON** blocks) with a Fortran-90 module and explicit allocation (using **ALLOCATE** and **SAVE**) of these arrays at the start of the model run. This allows us to tailor the size of the arrays to fit exactly the number of radial points handled by each individual node. This reduces both the storage requirements of the code on every node and, more importantly, it minimizes cache/TLB misses and page faults. In addition, it allows much larger calculations to be performed because the RAM, virtual memory and scratch disk space of every node can be fully utilized, thus effectively increasing the size of the possible calculation by the number of nodes.

We find that the use of adapted array sizes significantly improves the overall performance, even for a small number of processes. The scaling with more nodes has also improved considerably. However, the overhead of loops cannot be reduced and thus the speed-up cannot increase significantly if more nodes are used. We have verified with

a simple test program which only included one of the loops important for the radiative rate computation that this is indeed the case. Therefore, we conclude that further improvements cannot be obtained at the Fortran-90 source level but would require either re-coding of routines in assembly language (which is not practical) or improvements of the compiler/linker/library system. We note that these performance changes are very system dependent. For example, the serial “COMMON block” version of the code runs significantly (50%) faster than the serial “Fortran-90 module” version on both Cray’s or SGI’s, whereas on IBM RS/6000’s we found no noticeable difference in speed. This stresses that raw CPU performance is irrelevant as long as it is not supplemented by adequate compilers.

We also ran tests on the HP J200 machine, see Table 3. We use the public domain MPICH implementation of MPI compiled on this machine with its default compiler options. There is no full-F90 compiler available from Hewlett-Packard for this machine, therefore, we had to use the “COMMON block” version of the code. Therefore, the speed-ups cannot be expected to be optimal. However, a total speed-up of about 1.5 is acceptable. The speed-up for the opacity part of the NLTE calculation is a factor of 1.7, somewhat better than the factor of 1.4 achieved for the NLTE rate calculations. This is probably due to the fact that the rate computation is much more memory access dominated than the more floating point intensive NLTE opacity calculations.

7. Performance for realistic full model calculations

7.1. Supernovae

In order to test the performance of the parallel code in a practical application with velocity fields we calculated a supernova atmosphere model with parameters typical for a Type Ia supernova explosion. The total number of wavelength points = 48397, the

total number of levels treated in NLTE = 3752, and the total number of primary NLTE transitions = 16594, the number of secondary NLTE transitions = 184943, and the number of LTE lines=2346474. Fig. 3a displays the wall-clock time for a single model iteration as a function of processors and Fig. 3b shows the speed-up, which in agreement with our above results scales roughly as $N_{\text{node}}/2$. While this is significantly below the theoretical maximum of N_{node} scaling, it is a significant speed-up for practical applications.

7.2. Central stars of nova systems

To investigate the performance gains for a realistic stellar model at higher temperatures, we ran a complete NLTE model calculation for a set of parameters expected for the primary component of a nova system in a quiet post-outburst phase. The parameters appropriate for these white dwarf systems are $T_{\text{eff}} = 21,000$ K, $\log(g) = 8.0$ and solar abundances. We use the following NLTE species: H I-II, He I-III, C I-IV, N I-VI, O I-VI, Mg II, Ca II, S II-II, Si II-III, Ne I, and Fe II with a total of 2,826 NLTE levels and 26,874 NLTE lines. All NLTE lines are treated with detailed Voigt profiles. In addition, we include 621,920 LTE background lines and the calculation uses a total of 93,619 wavelengths points. On a **SGI Power Indigo 2** a single model iteration with this setup requires about 9.5h CPU time and the full model run (10 iterations) needs about 2 days CPU time. On 10 processors of the **IBM SP2** (using a standard load-distribution not optimized for the model parameters), a single iteration takes about 1.4h wall-clock time and the full model calculation needs about 7.3h wall-clock time, which is *less* than the CPU time for a *single* iteration on the **SGI Power Indigo 2**. This shows that the parallel speed-ups that we can achieve in realistic calculations are very significant, even with a small number of CPU's. With about 7.5h wall-clock time for a complete model iteration, substantial grids of these models can be constructed in relatively short time, thus making detailed analysis of observed spectra with

the best input physics feasible.

7.3. M dwarfs

We have run a realistic NLTE M dwarf test calculation with the following model parameters: $T_{\text{eff}} = 2700$ K, $\log(g) = 5.0$, and solar abundances. As NLTE species we include H I (10 levels), Na I (3 levels), Ti I (395 levels), Ti II (204 levels), C I (228 levels), C II (85 levels), N I (252 levels), N II (152 levels), O I (36 levels), and O II (171 levels), for a total of 1591 levels and 15062 primary NLTE lines (treated in detail with individual Voigt profiles). We use 113,433 wavelength points and include 288,775 background atomic LTE lines (with 28,011 of these are strong enough to be included with individual Voigt profiles) as well as 12,861,979 molecular LTE lines (including 3,753,353 with Voigt profiles).

In Table 4 we give the wall-clock times for one iteration on the IBM SP2. We have used a “small” code configuration with blocksizes appropriate for machines with about 128MB RAM per node although the test machine had up to 300 per node paging space and we used very large search windows for the atomic, molecular and NLTE lines in order to obtain a “worst case” scenario. Table 4 shows that the calculation is dominated by the LTE atomic and molecular line opacity whereas the NLTE opacities and rates are only a second order contribution to the total time per iteration. The scaling of the calculation is, therefore, very good up to the largest configuration that we have tested. We could not run the test model on a single IBM SP2 CPU due to both wall-clock time and memory restrictions, this demonstrates the importance of parallelization for practical applications.

There are possibilities to reduce the wall-clock time by, e.g., using larger blocksizes and a specially tuned load-distribution. The last IBM SP2 entry in Table 4 shows that an alternative load distribution can easily improve the overall speed although now some of the

sub-tasks require more wall-clock time.

We also include the timing results of the test run that we obtained on a single processor of a Cray C90 (CPU times). The Table shows that the C90 is about as fast as 5 nodes of the IBM SP2, which is roughly the relative performance ratio of a single IBM SP2 node to a single C90 processor. The wall-clock time on the C90 was much worse than on the IBM SP2, due to the time-sharing operation of the C90 CPUs.

8. Conclusions

We have been able to obtain a significant speed-up of our serial model atmosphere code with only a modest number of changes. We find that using the MPI library calls and a distributed memory model the parallel version of PHOENIX was easier to add to our existing serial code than a shared memory model where we have to carefully make sure that specific memory locations are only updated correctly. The speed-ups we have been able to achieve are below the theoretical maximum, however, this is not unexpected when such things as loop overhead and communications are accounted for. This is very similar to the earlier process of moving from strictly serial codes to vectorized codes, the theoretical maximum vector speed-up is very rarely reached in practical applications. The parallel speed-up of PHOENIX is important for practical application and, in addition, allows both much larger (in terms of memory size and CPU time) problems to be handled.

Future improvements of the parallel version of PHOENIX will include the distribution of the NLTE groups to different nodes (improving the degree of parallelization and allowing much larger problems to be handled on machines with less memory per node, e.g, the Cray T3D) as well as additional optimization of the code based on experience with large scale production runs on parallel machines.

It is a pleasure to thank D. Branch, P. Nugent, A. Schweitzer, S. Shore, and S. Starrfield for stimulating discussions. We thank the anonymous referee for suggestions which improved the presentation. This work was supported in part by NASA LTSA grants NAGW 4510 and NAGW 2628 and by NASA ATP grant NAG 5-3067 to Arizona State University and by NSF grant AST-9417242, and by an IBM SUR Grant to the University of Oklahoma. Some of the calculations presented in this paper were performed at the Cornell Theory Center (CTC), the San Diego Supercomputer Center (SDSC), supported by the NSF, and the Paderborn Center for Parallel Computing, we thank them for a generous allocation of computer time.

References

Allard, F., & Hauschildt, P. H. 1995, *ApJ*, 445, 433

Baron, E., Hauschildt, P. H., Nugent, P., & Branch, D. 1996, *MNRAS*, 279, 779

Gropp, W., Lusk, E., Doss, N., & Skjellum, A. 1996. MPICH Model MPI Implementation Reference Manual. Technical report, Argonne National Laboratory, Argonne

Hauschildt, P. H. 1992, *JQSRT*, 47, 433

Hauschildt, P. H. 1993, *JQSRT*, 50, 301

Hauschildt, P. H., & Baron, E. 1995, *JQSRT*, 54, 987

Hauschildt, P. H., Störzer, H., & Baron, E. 1994, *JQSRT*, 51, 875

Hauschildt, P. H., Starrfield, S., Shore, S. N., Allard, F., & Baron, E. 1995, *ApJ*, 447, 829

Hauschildt, P. H., Baron, E., Starrfield, S., & Allard, F. 1996, *ApJ*, 462, 386

Message Passing Interface Forum 1995. MPI: A Message-Passing Interface Standard, Version 1.1, Knoxville, TN: Univ. of Tennessee

Mihalas, D., & Mihalas, B. W. 1984. Foundations of Radiation Hydrodynamics, Oxford: Oxford University

Olson, G. L., & Kunasz, P. B. 1987, JQSRT, 38, 325

Rybicki, G. B., & Hummer, D. G. 1991, A&A, 245, 171

Schweitzer, A., Hauschildt, P. H., Allard, F., & Basri, G. 1996, MNRAS, submitted

Table 1a. Results of radiative transfer tests.

Test with 128 radial points				
nodes	IBM SP2	GC/PP	HP J200	
1	306.4 : 1.0	1410.6 : 1.0	818.8 : 1.0	
2	159.7 : 1.9	776.4 : 1.8	652.8 : 1.3	
3	108.0 : 2.8	590.2 : 2.4		
4	94.8 : 3.2	512.1 : 2.8		
8	63.8 : 4.8			
16	53.3 : 5.7			
32	56.1 : 5.5			
64	68.1 : 4.5			

Note. — The results are given in the format $t : x$ where t is the absolute wall-clock time in seconds and x is the speed-up factor relative to the serial run, rounded to 2 significant figures.

Table 1b. Results of radiative transfer tests.

Test with 50 radial points				
nodes	IBM	SP2	GCel	GC/PP
1	72.8 : 1.0	5057.0 : 1.0	164.1 : 1.0	
2	45.1 : 1.6	2473.1 : 2.0	117.1 : 1.4	
4	33.0 : 2.2	1447.0 : 3.5	107.0 : 1.5	
8	31.1 : 2.3	959.9 : 5.3		
16	34.5 : 2.1	754.8 : 6.7		
32	42.6 : 1.7	741.5 : 6.8		
64	62.9 : 1.2	907.7 : 5.6		

Table 2. Results of the line routine parallelization tests.

nodes	atomic lines	molecular lines	total time	IO time
IBM SP2 PIOFS				
1	1570.0 : 1.0	952.0 : 1.0	2790.0 : 1.0	87.4 : 1.0
2	802.0 : 2.0	654.0 : 1.5	1740.0 : 1.6	49.8 : 1.8
*2	769.0 : 2.0	539.0 : 1.8	1520.0 : 1.8	73.9 : 1.2
4	425.0 : 3.7	275.0 : 3.5	974.0 : 2.9	26.6 : 3.3
*4	388.0 : 4.0	304.0 : 3.1	899.0 : 3.1	67.2 : 1.3
5	352.0 : 4.5	233.0 : 4.1	861.0 : 3.2	21.7 : 4.0
10	193.0 : 8.2	124.0 : 7.7	582.0 : 4.8	10.4 : 8.3
20	114.0 : 13.8	82.7 : 11.5	470.0 : 5.9	7.1 : 12.2
IBM SP2 standard				
5	331.0 : 4.8	442.0 : 2.2	1170.0 : 2.4	206.0 : 0.4
Cray C90				
1	276.0	175.0	535.0	

Note. — The results are given in the format $t : x$ where t is the absolute wall-clock time in seconds and x is the speed-up factor relative to the serial run. We include also a run done without using the PIOFS filesystem. The entries marked with “*” have been obtained on the IBM SP2 of the University of Oklahoma, which has more RAM per node than the CTC machine. The longer I/O time on the OU machine may be related to the fact that both PIOFS and NFS mounts use the high speed switch on this machine.

Table 3. Results of the NLTE routine parallelization tests.

nodes	NLTE opacity	NLTE rates	total
IBM SP2			
1	13701.0 : 1.0	7015.3 : 1.0	21497.0 : 1.0
2	7234.3 : 1.9	3834.2 : 1.8	11860.0 : 1.8
5	3562.0 : 3.8	1987.2 : 3.5	6376.3 : 3.4
10	2479.4 : 5.5	1540.4 : 4.6	4844.2 : 4.4
25	2133.1 : 6.4	1257.6 : 5.6	4240.2 : 5.1
HP J200			
1	16102.0 : 1.0	11525.0 : 1.0	28554.0 : 1.0
2	9520.7 : 1.7	8458.4 : 1.4	19342.0 : 1.5

Note. — The results are given in the format $t : x$ where t is the absolute wall-clock time in seconds and x is the speed-up factor relative to the serial run.

Table 4. Results of a M dwarf model run including NLTE effects.

	atomic nodes	molecular lines	NLTE lines	NLTE opacity	total rates	time
IBM SP2						
2	13900.0	6340.0	2060.0	760.0	24900.0	
5	5740.0	2680.0	1100.0	519.0	11800.0	
10	3160.0	1300.0	912.0	505.0	7980.0	
20	1670.0	700.0	791.0	420.0	6140.0	
*20	1530.0	638.0	1280.0	646.0	5560.0	
Cray C90						
1	4900.0	2290.0	1270.0	943.0	10100.0	

Note. — The results are given are the absolute wall-clock time in seconds for the IBM SP2 and CPU times in seconds for the C90. The last table entry for the IBM SP2 (marked with a “*”) uses a more optimized load distribution that separates tasks. The results in a speed-up of 10% compared to the ‘simple’ load distribution.

9. Figures

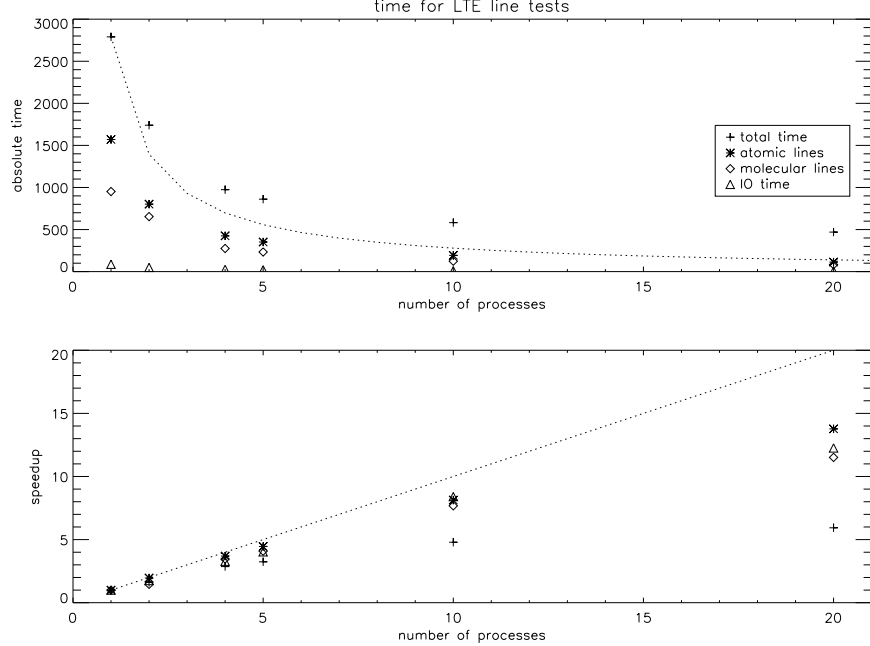


Fig. 1.— The speed-up and scaling of the line opacity calculation using PI0FS for different numbers of IBM SP2 nodes used. The upper panel with the wall-clock time (in seconds) used for the test calculations, the lower panel the speed-up factors. The dotted curves give the expected maximum parallel speed-up.

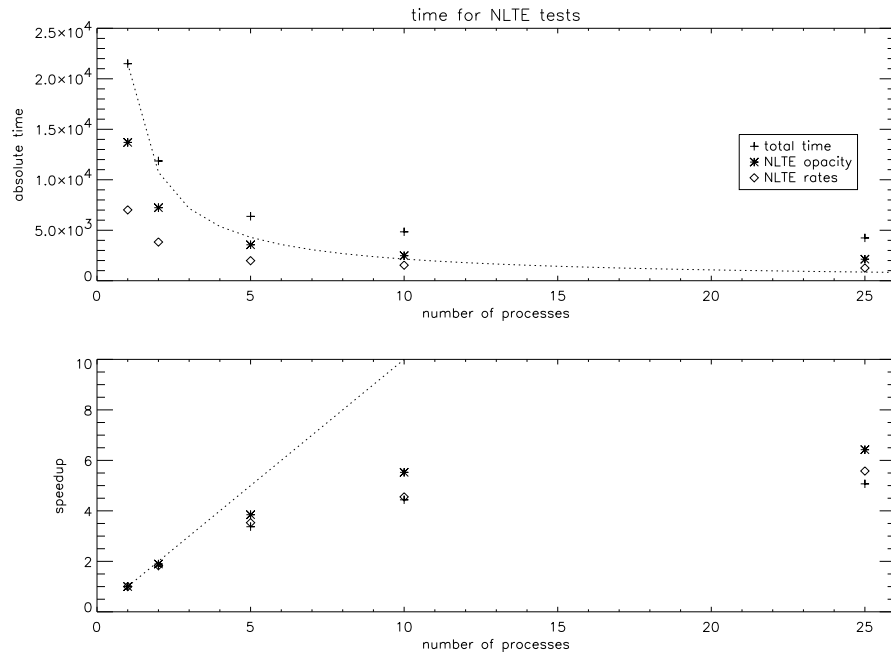


Fig. 2.— The speed-up and scaling of the NLTE parallel algorithm using Fortran-90 MODULEs and individual array allocation for different numbers of IBM SP2 nodes used. The upper panel with the wall-clock time (in seconds) used for the test calculations, the lower panel the speed-up factors. The dotted curves give the expected maximum parallel speed-up

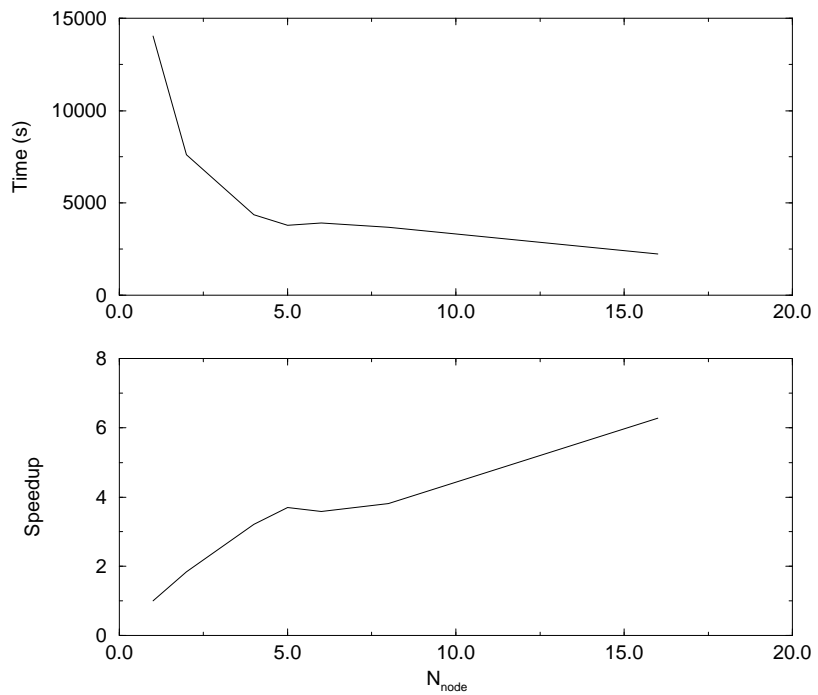


Fig. 3.— The speed-up and scaling of the NLTE parallel algorithm for a practical application for different numbers of IBM SP2 nodes used. The upper panel with the wall-clock time (in seconds) used for the calculations, the lower panel the speed-up factors.